

EFFECT OF SYNCHROTRON RADIATION IN THE PROPOSED  
4 GEV ARGONNE MICROTRON**MASTER**E. A. Crosbie  
Physics Division  
Argonne National Laboratory  
9700 S. Cass Avenue  
Argonne, IL 60439

CONF-830311--177

DE83 014294

Introduction

Synchrotron radiation in the sector magnets of the 4-GeV microtron designed at the Argonne National Laboratory produces a small but noticeable distortion of the closed orbits of the system and a very-significant growth of the horizontal and longitudinal phase-space emittances. Because of the small apertures in the three 25-meter linacs, it is important that the expected growth of the beam be calculated as accurately as possible.

For this reason, a computer program has been written which follows the motions of individual electrons in the four dimensional horizontal and longitudinal phase space as they are accelerated in the system. As the electrons go through the sector magnets, they emit quanta at random with randomly chosen energies. The final results show 63% emittance (area/ $\pi$ ) values of 0.15 mm mrad and 630 keV degrees for the horizontal and longitudinal phase spaces respectively. The 99% values are about 4.6 times larger.

Brief Description of the  
Argonne Microtron Design

The Argonne microtron is adequately described by other reports at this conference. For the purposes of this paper, we call attention to the fact that there are 3 long 28 m linac sections separated by sector magnets from 3 dispersion sections where the orbits for different energies are separated. The radius of curvature in the sector magnet is proportional to the energy,

$$r = 3.2855E \text{ m/GeV.} \quad (1)$$

The interaction of the linac rf systems with the synchrotron energy loss in the sector magnets produces different orbit effects in the downstream and upstream linac sector magnets. We shall call these sector magnets SM1 and SM2 respectively. The optical systems on each of the orbits in the dispersion sections are designed to produce zero dispersion in the linac straight sections. This condition produces a general horizontal transfer matrix<sup>1</sup> for the dispersion straight section orbits that is independent of the focusing elements actually used to achieve the conditions.<sup>2</sup> The distorted orbits shown in the next section therefore show gaps between the exits of SM1 and the entrances to SM2.

Closed Orbit Distortions Caused by  
Synchrotron Radiation Energy Loss

The average synchrotron radiation energy loss per sector magnet is given by<sup>3</sup>

$$\Delta E = \frac{C}{6r} E^4 = 4.489 E^3 \text{ keV/GeV}^3 \quad (2)$$

where  $C = 88.5 \text{ m keV/GeV}^4$  and  $r$  has been replaced by eq. 1. The phase error must slip to make up for the energy loss in the two sectors. From the linac focusing condition one finds that the amount of this slip is

$$\delta\theta = -.768 E^3 \text{ mrad/GeV}^3 = -50 \text{ mrad at 4 GeV} \quad (3)$$

For the steady state condition (which doesn't actually exist), the energy error must change from  $-\Delta E$  at the linac entrances to  $\Delta E$  at linac exits. Therefore the beams have a net positive energy error in SM1 and a net negative error in SM2. This produces in the next linac section a displacement vector which must be compensated for by an initial horizontal phase space vector in the previous linac section to produce a closed orbit. The steady state solution turns out to be a vector with zero displacement and negative slope that increases with energy. At 4 GeV the magnitude of this slope is about 0.1 mrad producing  $\pm 1.2 \text{ mm}$  of displacement at the upstream and downstream ends of the linac respectively.

The dynamical problem has been solved using a computer program. The four dimensional phase point is started at 0 at 185 MeV. It gains energy in the linacs and loses energy in the sector magnets at a constant rate. The resulting horizontal distortion is shown in the phase space plot in Fig. 1 (Only the last 30 linac passes are shown.) The displacement is negative in SM1 and positive in SM2.

These orbit distortions are caused by the fact that the original microtron design does not properly account for the interaction of the rf system with the synchrotron radiation loss. Since the energy error is positive in SM1 and negative in SM2, clearly more bend is required in SM1 than in SM2. Also the optical axes in the dispersion sections must have a negative slope.

When one adds compensating positive and negative bends to the upstream and downstream ends of properly tilted optical axis in the dispersion straight sections all of the orbits can be made to stay on the center lines of the linacs. The longitudinal phase space motion after making these corrections is shown in Fig. 2. The required displacements and bends required to remove the orbit distortions are small and have values of  $\pm 0.3 \text{ mm}$  and  $\mp 0.013 \text{ mrad}$  at 4 GeV.

**NOTICE****PORTIONS OF THIS REPORT ARE ILLEGIBLE.**

It has been reproduced from the best available copy to permit the broadest possible availability.

\* Work supported by the U. S. Department of Energy under Contract W-31-109-Eng-38.

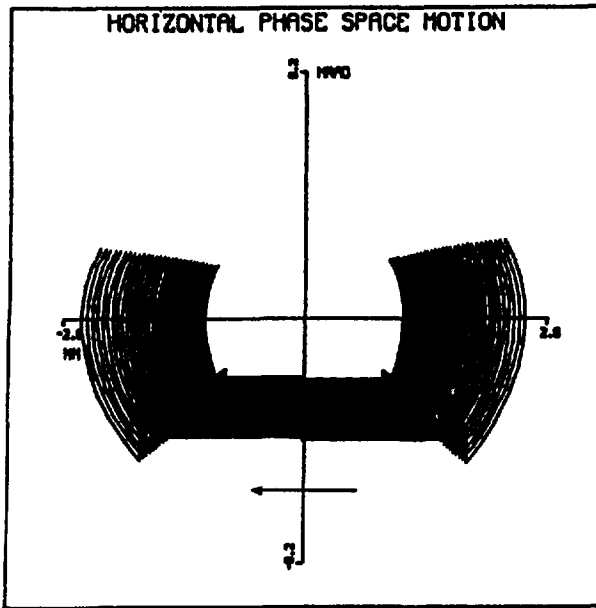


Fig. 1 Phase space plot showing the horizontal orbit distortions caused by synchrotron radiation (last 30 turns).

Longitudinal and Horizontal Phase Space Growth

To study the growth of the phase space areas due to quantum fluctuations, a computer program has been written that follows the four dimensional phase space behavior of many particles as they are accelerated in the microtron from 180 MeV to 4 GeV. The initial phase space points are chosen at random from exponential phase space area/2 $\pi$  distributions having 90% values of 0.05 mm urad horizontally and 90 keV deg longitudinally. As the particles are accelerated and go through the sector magnets, they lose energy in a random manner as described below.

The average number of quanta emitted per unit angle is given by<sup>3</sup>

$$\frac{dN}{d\theta} = 19.8 E/\text{GeV} \quad (4)$$

The critical photon energy  $u_c$  is defined as

$$u_c = 0.7031 E^2 \text{ keV/GeV}^2 \quad (5)$$

Defining  $\xi = u/u_c$ , where  $u$  is the photon energy, the probability that  $\xi$  will be found between  $\xi$  and  $\xi + d\xi$  is given by<sup>3</sup>

$$F(\xi)d\xi = \frac{3}{5\pi} \int_{\xi}^{\infty} K_{5/3}(\xi') d\xi' \quad (6)$$

where  $K_{5/3}$  is a modified Bessel function. For random selection of the photon energies, one requires the inverse of the distribution function<sup>4</sup>

$$G(t) = \int_0^t F(\xi)d\xi$$

$$= 1 - \frac{3}{5\pi} \int_0^{\infty} e^{-t \cosh(x)} \text{sech}^2(x) \cosh\left(\frac{5x}{3}\right) dx \quad (7)$$

$G(t)$  has been calculated numerically and polynomial and exponential fits over small regions were generated to give the inverse function.

Each sector magnet is divided into 10 subsections. To approximate the randomness of the photon emission the actual number of emitted photons for each electron in the subsection is chosen randomly from a Poisson distribution. (This random choice of the number of photons per subsection adds about 30% to the phase space growth rates.) The energy of each photon is chosen from a random number and the inverse of  $G(t)$ . The total of the photon energies for each particle is the energy loss for that particle in the subsection. The particles are then transformed to the next subsection, taking into account their new energy error terms. The phase error changes are calculated from the integral of the changed displacements. Damping of the oscillations is provided for in the linac sections.

The program has been run a number of times with 500 particles. Typical results are shown in Fig. 3, 4, 5. The centers of the distributions follow the expected closed orbits distortions very closely. The growth rates are independent of whether or not the tilted dispersion system is used.

The moments shown in Figures 3 are calculated after first subtracting the expected average positions. For exponential distributions these should correspond to 63%, 76%, 84% and 89% of the beam. The results for  $\langle t \rangle$  are about .15 mm urad for the horizontal phase space and 630 KeV degrees for the longitudinal phase space at 4 GeV. The 99% levels should be 4.6 times larger.

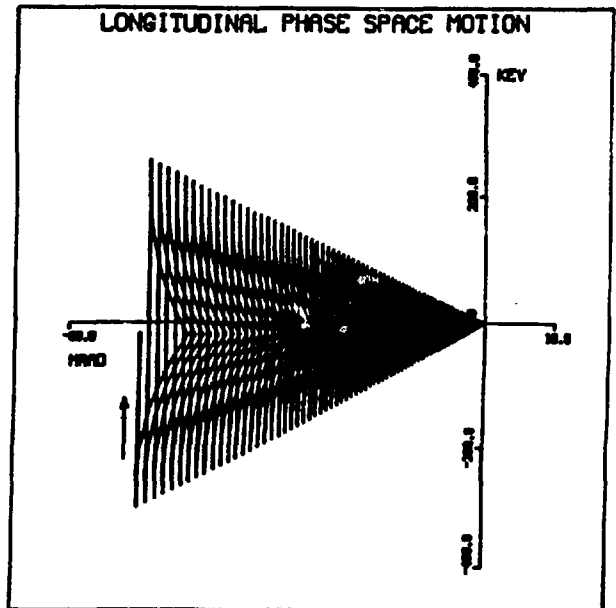


Fig. 2 Longitudinal phase space errors with horizontal orbit distortions removed.

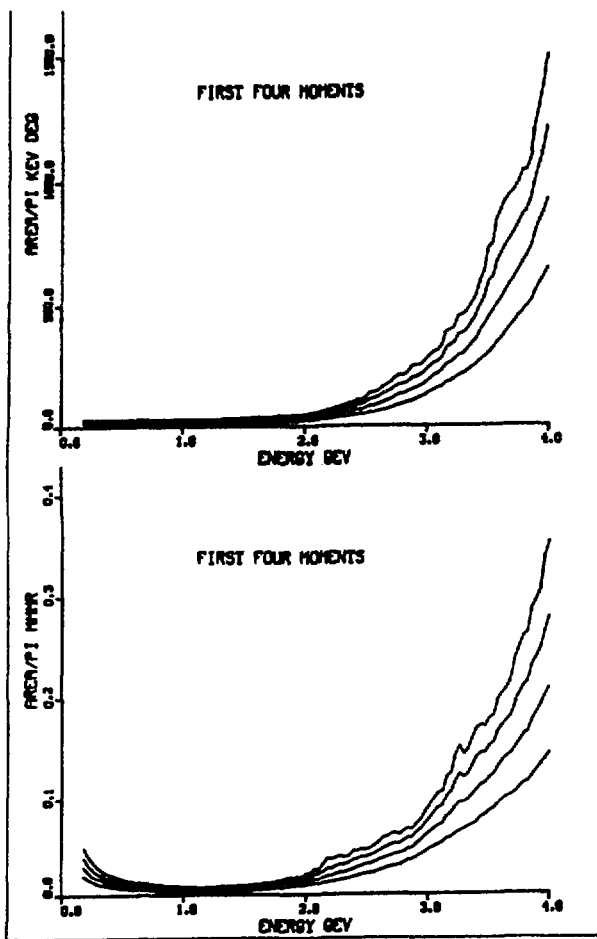


Fig. 3 Growth of the phase space  
Top: Longitudinal, Bottom: Horizontal

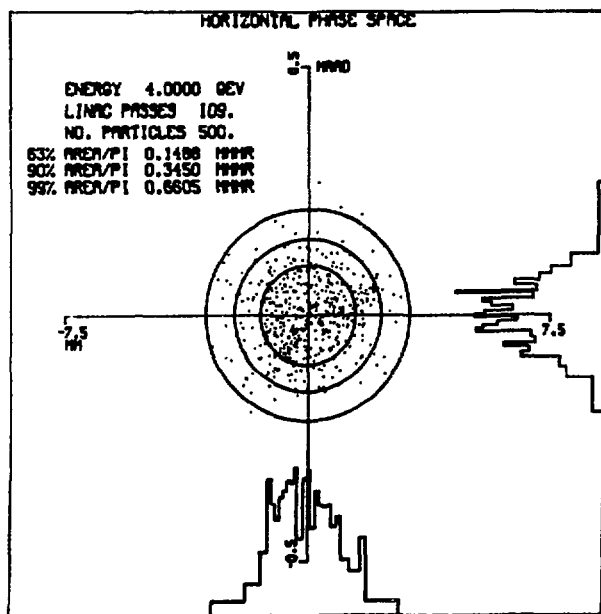


Fig. 4 Final distribution of the 50° horizontal phase space points at 4 GeV.

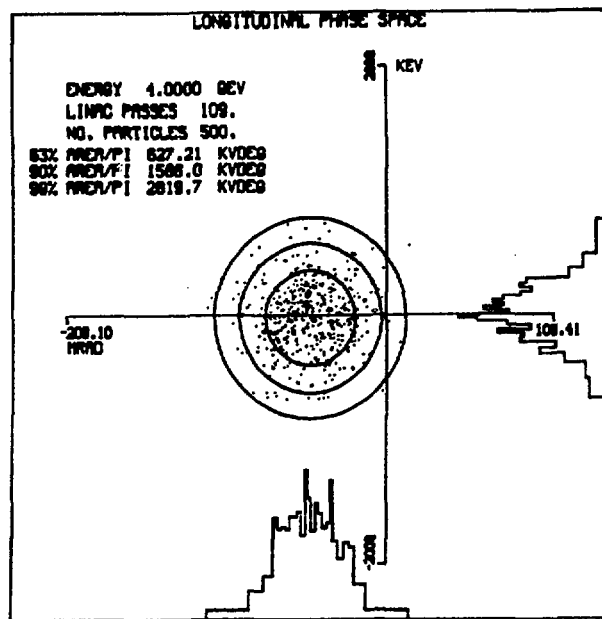


Fig. 5 Final distribution of the 500 longitudinal phase space points at 4 GeV.

#### Acknowledgment

The author wishes to give special thanks to W. J. Cody of the Argonne Applied Mathematics Division for supplying the representation of the photon energy distribution function (shown in equation 7) and for writing the special computer subroutine that gave numerical results.

#### References

1. E. A. Crosbie, Restraints on the Linac-to-Linac Horizontal Phase Advance in Recirculating Microtrons ANL-GEM-31-83.
2. E. Colton, Transverse Beam Containment in the ANL 4 GeV Microtron. F 20 this conference.
3. M. Sands, The Physics of Electron Storage Rings, SLAC 21.
4. W. J. Cody, Private communications, see acknowledgements.

## **DISCLAIMER**

**This report was prepared as an account of work sponsored by an agency of the United States Government. Neither the United States Government nor any agency thereof, nor any of their employees, makes any warranty, express or implied, or assumes any legal liability or responsibility for the accuracy, completeness, or usefulness of any information, apparatus, product, or process disclosed, or represents that its use would not infringe privately owned rights. Reference herein to any specific commercial product, process, or service by trade name, trademark, manufacturer, or otherwise does not necessarily constitute or imply its endorsement, recommendation, or favoring by the United States Government or any agency thereof. The views and opinions of authors expressed herein do not necessarily state or reflect those of the United States Government or any agency thereof.**